Forward looking clear air turbulence measurement with the AWIATOR LIDAR sensor

Nikolaus Peter Schmitt, Wolfgang Rehm, Thomas Pistner, Hermann Diehl, Peter Navé (1)
Guillermo Jenaro-Rabadan, Pierre Mirand, Mael Reymond (2)

(1) EADS Innovation Works
85521 Muenchen, Germany
nikolaus.schmitt@eads.net

(2) AIRBUS SAS
316 Route de Bayonne
31060 Toulouse CEDEX 9, France

1. Introduction

The accurate measurement of the airflow in front of an air vehicle is an important function for modern high performance military and civil airplanes and helicopters. For military aircraft, a good knowledge of the true 3D airspeed vector is an essential quantity for the flight control system, especially for thrust vector control. In civil aircraft, the measurement of gust, turbulences and wake vortices and the counteraction against them by a feed-forward flight control system would, firstly, alleviate structural loads and therefore extent the life time of the structure; secondly, further increase passenger safety in turbulence; and thirdly, provide a higher passenger comfort.

A unique LIDAR onboard sensor was developed and flight tested using a direct detection short pulse UV Doppler LIDAR. This detection schemes allows measurements even in aerosol-depleted air at distances of 50m, which is necessary for reliable and high-frequency measurements of clear air turbulence at cruise altitude. A fringe-imaging technique was used applying an intensified CCD camera, allowing fast gating for longitudinal measurement volume reduction (as necessary for real-time control purposes) and in-flight re-calibration by image processing. Algorithms have been developed and applied to determine the wind speed at m/s accuracy.

This paper describes first results achieved in flight tests using an Airbus A340-300 aircraft with the forward looking direct detection LIDAR to measure turbulences ahead, which was integrated in a fairing below the aircraft nose.

The research has been partly funded by the European Commission within the AWIATOR project [1].

2. Sensor principle

The sensor must be capable of measuring molecular (Rayleigh) and advantageously in addition aerosol (Mie) scattering, while ensuring reliable operation under pure Rayleigh backscatter conditions. The required forward looking distance is >= 50m, the update rate 60Hz per measurement or 15Hz for the full vector, the longitudinal accuracy +/-15m and the required wind speed accuracy around 1 m/s along the line-of-sight.

The wavelength shift is measured by a Fabry-Perot interferometer; difference frequency measurement as used in coherent detection is not applicable for Rayleigh scattering due to the broad spectrum of scattered light due to Doppler-broadening caused by Brownian motion: The required accuracy of about 1m/s for the detected signal corresponds to a frequency shift of ~6MHz at the selected UV wavelength of a signal with a spectral width of ~3GHz which corresponds to a Doppler broadening of 600m/s. Therefore, the frequency shift of the entire detected broadband signal has to be measured with a relative precision of about 1/600. The shape of the spectrum also depends on parameters such as temperature, air pressure and aerosol concentration. For obtaining the full 3D wind speed vector the Doppler shift must be determined in at least three directions. In our case four directions were used for redundancy reasons (fig.1).

The system consists of a single-frequency frequency-tripled Nd:YAG laser; a scanning system for beam multiplexing; an optical system for beam transmission and reception; a receiving demultiplexer; a Fabry-Perot interferometer; an image-intensified CCD camera; a data recording and real-time data processing unit; and control electronics.

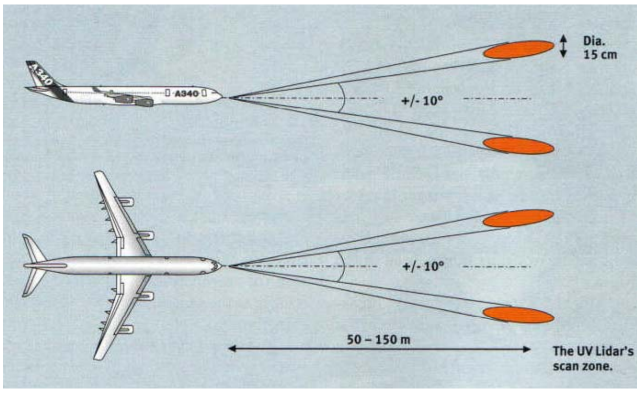

Fig. 1: Measurement geometry.

The LIDAR sensor was realised in two phases. In stage 1 a flight-worthy system was built capable of looking ahead 35m in order to prove the feasibility of the principle. This was flight-tested in 2004. Stage 2 of the system was flight tested in 2006. It consists, in addition to stage 1, of an upgraded laser at 10 times the output power and more than 10 times the optical receiver efficiency.

The laser (see sensor head in fig. 2) is a single-frequency, third-harmonics Nd:YAG operating at 355nm, with 300mW for stage 1 and 3W for stage 2. It emits pulses of ~10ns width at kHz rates. It was developed within this project by EADS because suitable devices were not available on the market.

The laser beam is multiplexed in four directions by a scanning system patented by EADS, which generates a stable focus at the four positions. A full scan is completed at a rate of 15Hz. In the receiver path the backscattered photons are focussed into four UV-fibres and multiplexed by a rotating mirror into one fibre that is connected to the receiver box. The Fabry-Perot etalon has a finesse of about 5. Its function is to generate circular interferogrammes. The change in the radius of the circular interferogrammes is directly proportional to the change of wavelength due to the Doppler shift, corresponding directly to the change in relative speed of the airflow.

The imaging system consists of a modified DiCAM Pro CCD camera with an UV sensitive microchannel plate. The sensor has 640×480 pixels; electronic on-chip binning is used.

The data recording and processing unit was specified by EADS; design and manufacture were contracted to Nallatech [2]. Camera data are transferred to the unit by optical transceiver/receiver interface technology. Both the recording and the processing system are based on Xilinx Virtex II FPGAs for highly parallel throughput and image processing.

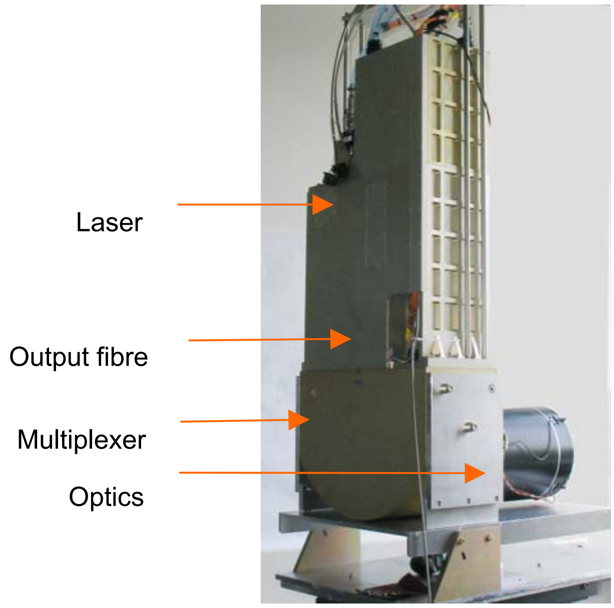

Fig. 2: Sensor head

3. Theoretical model and evaluation strategy

The backscattered laser light generates, after passing through the etalon, the well-known circular interference pattern, following an Airy function.

In practice, this function must be modified: The thermal broadening due to the Doppler shift caused by the Brownian motion has to be considered; this implies the convolution of the intensity $I(\lambda, \theta)$ with the Gaussian distribution of the one-dimensional speeds of the scattering particles, taking into account the mixture of molecules and aerosols. Also, artefacts of the optical system such as vignetting and an off-centre beam axis position must be modelled. In order to obtain the desired accuracy for the backscattered wavelengths, given the expected low photon counting rates, it is not sufficient to just estimate the position of the rings by simple geometrical considerations. These parameters have to be determined with sub-pixel accuracy. Therefore it is necessary to fit the above-mentioned modified Airy function with the unknown parameters to the data of the entire image plane. Data processing time poses a severe constraint.. Therefore, an algorithm was developed based on a more generic approach allowing data processing that is about 10-20 times faster than full parameter modelling. The algorithm is under patent filing and will be reported at a later date.

The system parameters, which are fairly constant over time, are determined by using a calibration signal. This calibration signal, generated by directly feeding the laser into the receiver, was used to determine the drift of both the laser and the etalon. The corrections determined are then used for compensating the drift of the measured atmospheric signal. Fringes measured under different conditions are shown in fig. 3.

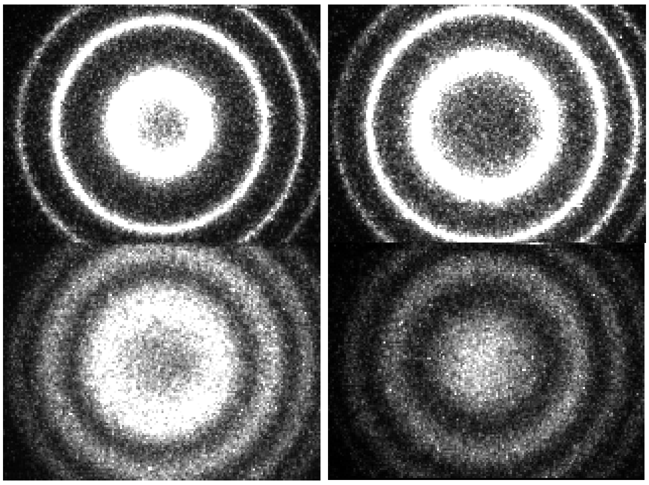

Fig. 3: Measured interferogrammes. Upper left: Reference signal. Upper right: Backscatter in dense clouds (nearly pure Mie). Lower left: Backscatter at 12,000ft altitude. Lower right: Backscatter at 39,000ft altitude (nearly pure Rayleigh).

4. Flight tests

Although the sensor development is aimed at direct forward control in modern fly-by-wire aircraft, due to several reasons the first flight experiments have been carried out without forward feeding in order to focus on the evaluation of the sensor. The LIDAR sensor was installed in a fairing beneath the cockpit of an A340-300 test aircraft of AIRBUS (fig. 4). The fairing included an UV transmissive window with antireflection coating for the laser wavelength. The centre of the sensor was in line with the aircraft x-axis (deviation below ~0.3°), thus the four measurement directions were 10° off to the aircraft's xy- & xz planes , or 14° in the diagonal.

Several flight tests with a total duration of more than 17 hours were performed. Different flight envelopes including flight levels up to 39,000 feet (see fig. 5) and speeds up to Mach 0.82 were covered. The weather conditions varied from clear air to dense clouds at various altitudes.

5. RESULTS

A preliminary evaluation of the data yielded the following results:

Interferogrammes could be recorded at all flight levels up to 39,000ft. At those altitudes, the aerosol backscatter signal is reduced by a factor 10^3 as compared to ground level, and therefore is a factor of $5*10^3$ weaker than the molecular signal. This proves that the sensor is able to perform in a purely molecular environment.

Sensor signals were also obtained in dense clouds where the visibility was less than 5m. The strong Mie scattering outweighed the effect of absorption of the laser beam by orders of magnitudes.

As has been proven in former flight tests [3], even in rain and ice good sensor signals were received. Because of the gated viewing, raindrops on the window did not disturb the measurement.

Fig. 4: Sensor installation in a fairing beneath the cockpit of the A340.

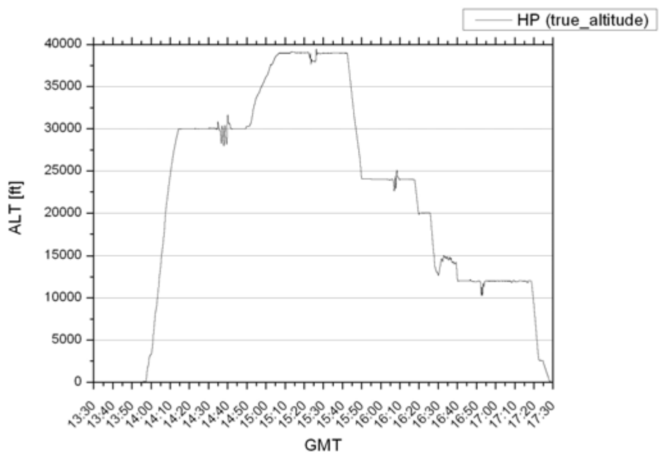

Fig.5: Flight altitude versus time of the flight test

Figure 6 displays sensor results obtained at high dynamic speed (colored noisy lines: LIDAR sensor data; smooth black line: a/c TAS sensor signal projected into the four lines-of-sight). It shows that the LIDAR sensor data track very well the dynamics of the aircraft.

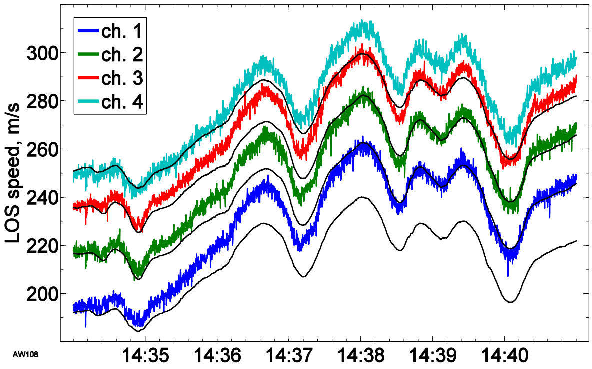

Fig. 6: Graph of the LIDAR sensor speed data in the four measurement directions (noisy, colored curves) and a/c sensor data (black curves). Curves shifted artificially 20 m/s apart for better visibility.

As can also been seen there is an offset between the TAS and the sensor data. This conspicuous offset was found to be not constant – sequences with large drift of the offset were found as well as some without. Analysis showed that the offset is a function of the fringe position and the fringe radius difference between reference and measured diameter, related to a reference signal "speed" and the measured speed. The reasons for this are 1.) vignetting of the fringe images, which is a radially decrease of intensity transmission of the etalon and the optical system, and 2.) distortions by spherical aberrations of the optical transfer system, both generating slight shifts of the fringe radius. By a very simple compensation this offset could be compensated. Inputs to the compenastion formula are the reference speed and the measured speed. The formula is valid only during the flight phase but not during the start phase. For the start phase an additional parameter reflecting the aerosol concentration has to be introduced. Fig. 7 indicates the remaining offset for the full flight. With the exception of the starting phase and a non-stabilized phase of some minutes around 15:20, the offset stayed below 5 m/s. Fig. 8 displays the same data as of fig. 6 after compensation of the offset.

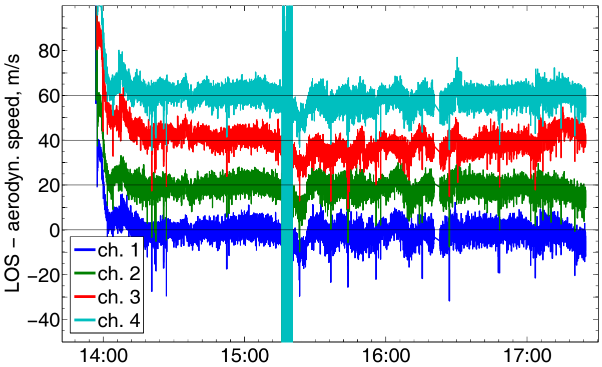

Fig. 7: Remaining offset after compensation (upshifted 20 m/s)

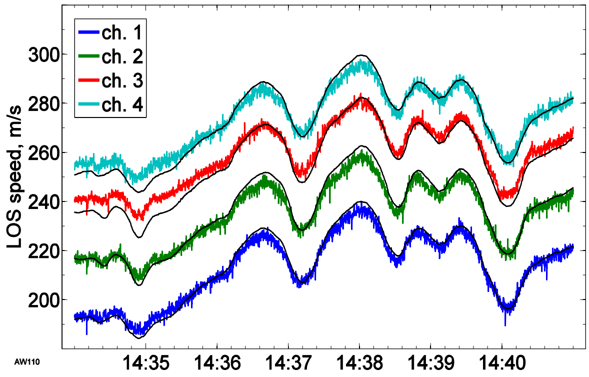

Fig. 8: Same data as in fig. 6 after offset compensation

Fig. 9 shows the standard deviation of the sensor data of the whole flight. The laser power decreased with time due to decreasing temperature inside the avionics bay where the laser was installed (fig. 10). Nevertheless, the FL 390 sequence had still moderately high laser power available. The standard deviation achieved ranged mainly between 1 m/s and 1.5 m/s.

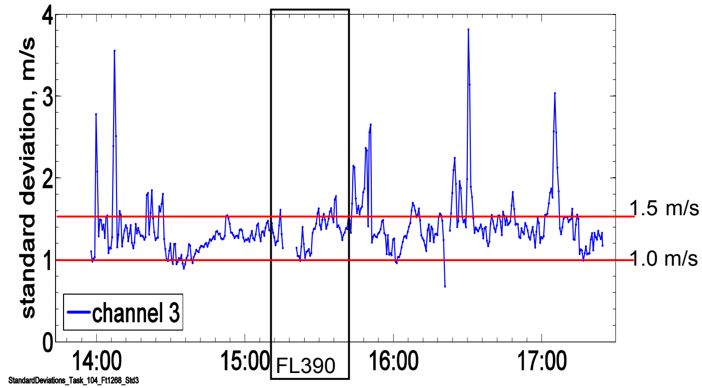

Fig. 9: Standard deviation of the sensor data during the whole flight (channel 3). FL390 marked by box.

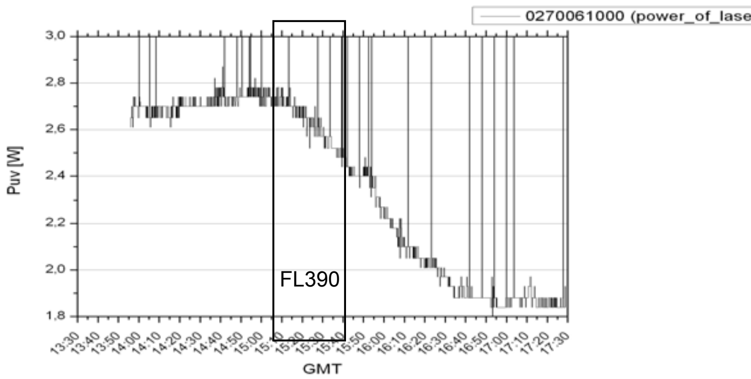

Fig. 10: Laser power versus time. Degradation occurred due to a temperature drop in the avionics bay by fairing cool-down. Outliers were caused by data transmission distortions.

The y- and z-components are then derived from LOS speed measurement differences as indicated below (fig. 11).

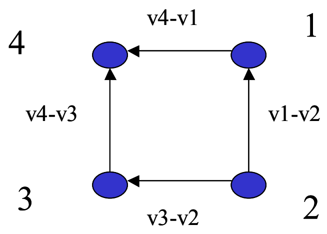

Fig. 11: Reconstruction of y- and z-speed components by LOS speed differences.

Typical examples of reconstructed y- and z-components are given in fig. 12 (upper two curves correspond to the y-components, lower two correspond to the z-component). The noisy curves are again the LIDAR data, the smooth curves the a/c data projected to the LIDAR axes. All curves are plotted 20 m/s apart for better visibility. The typical peaks in the z-component of the a/c data can be very well correlated with the LIDAR sensor data even in the unfiltered data of fig. 12, and much improved in fig. 13 in which the LIDAR data are filtered with a 0.25 Hz low-pass filter.

The two y- and the two z-components can be combined to a single y and a single z-component with standard deviation around 1.5 m/s for FL 390 as shown in fig. 14 (for the whole flight test).

It has to be noted that the y- and z-components given here have to be multiplied by a factor of 2.9 to calculate the y- and z-.components in the aircraft reference system (due to sine-projection of the LOS axes at given angle of +/- 10°).

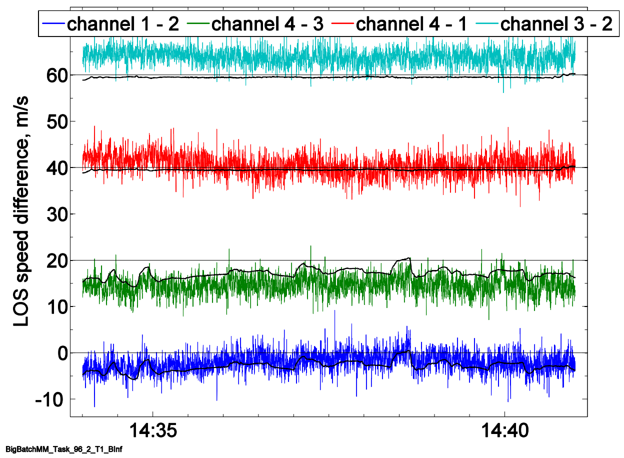

Fig. 12: y- component (upper two curves) and z-component (lower two curves) of LIDAR data (noise curves) and a/c data (solid curves) reconstructed from speed differences – unfiltered. Artificially shifted 20 m/s apart.

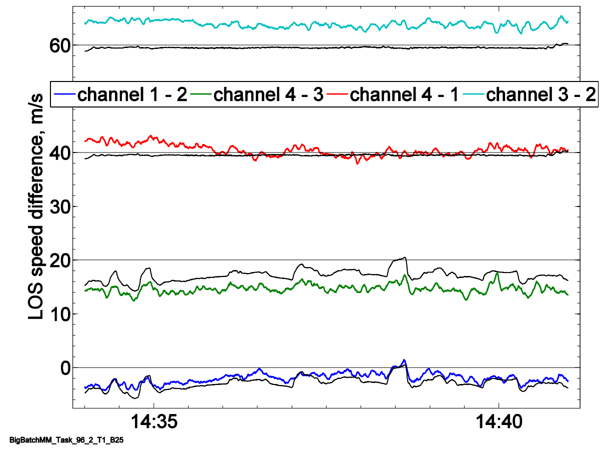

Fig. 13: Same as fig. 12, but filtered with 0.25 Hz.

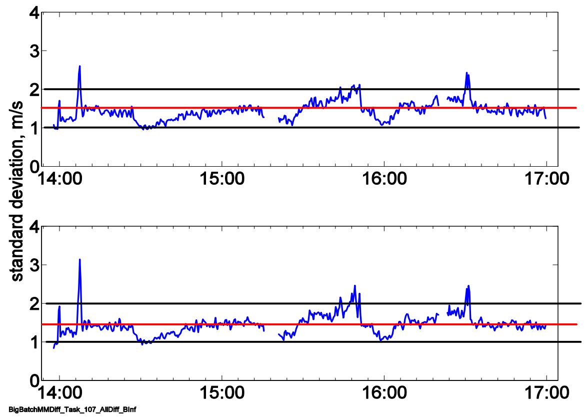

Fig. 14: Standard deviation of z-component (upper curve) and y-component (lower curve) of the LIDAR data.

Thus the 1.5m/s standard deviation of the y-and z-components result in ~4.5m/s in the a/c reference system. This factor 2.9 results from sin(beam angle 10°), divided by sqrt(2) (difference of two beams), and further division by sqrt(2) (adding left and right z- or upper and lower y-components, respectively).

The beam angle of 10° was chosen at the beginning of the project when a much longer measurement range was envisaged. During the AWIATOR project, the optimum measurement range was determined to be 50m ahead of the aircraft (which corresponds to about 74m from the center of the measurement volume to the wing edge of the A340), enabling a forward looking time of ~300ms. This is sufficient for flight control input and control surface deflection (about 5° at 40°/second deflection rate). A too long measurement range would result in erroneous turbulence counteractions due to the high dynamics of the turbulences. At the reduced forward measurement range of 50m, the beam angles could easily be increased to 35° or 45°, resulting in a projection factor of only 1.0 or 0.7 instead of 2.9, see figure 15. For example, at

45° and a factor of 0.7 (lower than 1 due to the addition of two z-components right/left hand resp. y-components upper/lower) an a/c y-z-standard deviation of 1 m/s can be achieved with the established LOS standard deviation of 1.5 m/s.

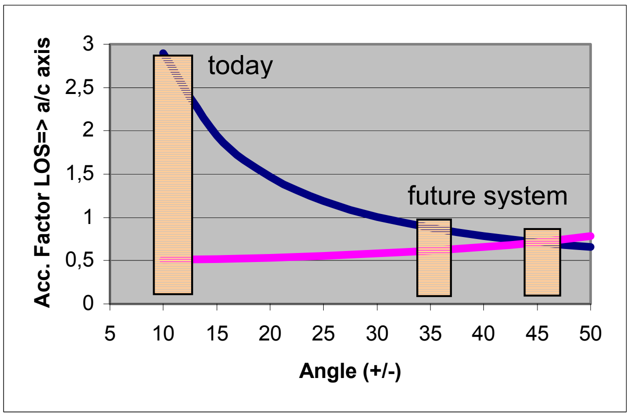

Fig. 15: Accuracy factor for computing the y- and z-components of the wind in the a/c reference system from the LOS speed differences as a function of the beam angles. Upper (blue) curve y,z-error factor, lower (purple) curve x-error factor.

6. Summary

A novel in-flight LIDAR sensor was designed, developed and for the first time flight tested in a forward looking configuration. It is based on a short pulse UV direct detection fringe imaging technique. It aims at measuring turbulences – even at high flight altitudes – ahead of the aircraft. Its ultimate objective is to feed-forward the aircraft flight control for active counteractions.

It was shown that the direct detection Rayleigh/Mie LIDAR is capable of detecting the wind speed under flight test conditions up to cruise altitudes, in clear air and in clouds. Standard deviations of the line-of-sight LIDAR signal as low as about 1.0-1.5m/s at an altitude of 39,000ft and measurement range of 54m have been achieved. The update rate was 60Hz for each LOS measurement (15Hz for full vector) and the measurement volume depth was +/- 15m.
It was proven that the LIDAR signal follows the reference aircraft speed measurement system very well. Derived y- and z-components of the signal have been measured with a standard deviation of about 1.5 m/s at FL 390 as well, to be multiplied by the geometric projection factor depending of the measurement beam axis angle with respect to the aircraft reference system. At the given non-optimum 10° beam angle set-up used in these flight tests for several reasons, the factor is about 2.9. In future configurations this angle can easily be increased to 35° or 45°, leading to a projection factor of 1.0 and 0.7, respectively (below 1.0 in the latter case because of the addition of two z-components at the left and the right of the a/c body resp. up/down for the y-component).
The data have been compared with aircraft true air speed sensor data that were projected onto the LOS directions of the LIDAR beam directions, utilizing aircraft attitude data. Very good correlation has been found. Offsets could be compensated statically and dynamically to below 5m/s in the lower aerosol concentration sequences (after aircraft take-off) for LOS components as well as y-, z-components.

The sensor features clear potential for future implementation in a real-time direct-feed-forward automatic flight control system for e.g. active gust load alleviation. It was found by detailed analysis within the AWIATOR project that a gust load alleviation of about 40% can be achieved, which leads to the conclusion that the maneuver loads will be the dominant limits in the future. A reduction of maneuver loads to 2.2g would allow to gather maximum benefits of gust load alleviation with the forward looking LIDAR sensor.

Expected standard deviations and the range for a future operational sensor are about 0.7-1.0m/s in the aircraft reference system and 50-250m in all-weather conditions as well as at high flying altitudes. Further benefits will comprise increases in the ride comfort and passengers' safety, e.g. negative-g prevention. A very interesting option would be to use the sensor for wake-vortex nearfield measurement.

In a next step, the full system capability will have to be proven in a fully integrated system test within the scope of a follow-on R&D project. It will feature the LIDAR sensor developed here integrated into the skin of the aircraft, rendering a fairing unnecessary, with real time data processing and direct feed forward to the flight control system.

Acknowledgements
The authors wish to acknowledge important contributions by Paul Zeller (laser development), Stephan Stilkerich (FPGA hardware platform and FPGA design), Guenther Reithmeier (mechanical design) and Klaus Schertler (valuable inputs to novel algorithms), all at EADS. Special thanks to Jens König, manager of the AWIATOR project, for excellent cooperation and support.

References
[1] http://www.awiator.net/project.html
[2] www.nallatech.com
[3] N. P. Schmitt et al.: Airborne direct detection UV LIDAR, 23rd Intern. Laser Radar Conf. ILRC 2006 Nara/Japan, p. 167-170